www.czasopisma.pan.pl PAN www.journals.pan.pl

ARCHIVES of FOUNDRY ENGINEERING

ISSN (2299-2944)
Volume 2025
Issue 1/2025

34 – 42

10.24425/afe.2025.153772

5/1

Published quarterly as the organ of the Foundry Commission of the Polish Academy of Sciences

Transmission Line Model Measurements of Metal-Semiconductor Contacts

M.M. Musztyfaga-Staszuk [a, *], P. Panek [b], A. Czupryński [a], C. Mele [c]

[a] Silesian University of Technology, Welding Department, Poland
[b] Institute of Metallurgy and Materials Science PAS, Poland
[c] Dipartimento di Ingegneria dell'Innovazione, Università del Salento, Italy
* Corresponding author: E-mail address: malgorzata.musztyfaga@polsl.pl

Received 04.07.2024; accepted in revised form 13.11.2024; available online 18.02.2025

Abstract

The intriguing aspect of the research involves acquiring experimental results related to engineering processes at low temperatures. One could mention the demonstrated relationship between the manufacturing method and the enhancement of the metallic component's quality by reducing the resistance at the junction between this front component and the substrate. Investigations were performed into two series of samples, which were applied to two experimental copper pastes for manufacture front metallization. The process of manufacturing front elements was performed at low temperature. The results of the electrical investigations were then compared to those obtained in a high-temperature range using commercial silver pastes. The temperature interval from 500 to 1000 °C can be considered typical for the thick-layer co-firing process, while temperatures lower than 200 °C can be considered typical for hetero-junction technology. TLM method can be used to collect data and information used in the technological process of their production. Based on the conducted experiments, it can be concluded that the test results obtained are comparable. The method of TLM transmission lines applied is of interest to various research centres, groups of specialists, and designers of measuring instruments dealing with monitoring changes in the values of electrical parameters.

Keywords: Transmission line model (TLM), Semiconductor structure, Front contact/metallization

1. Introduction

The metallization operation is one of the final operations of manufacturing a photovoltaic cell/semiconductor structures [1]. It requires the deposition and manufacturing of the front metallization with proper connection in the semiconductor material. When contacts are established, extra resistances are introduced into the electrical circuit, which restricts the flow of photocurrent [2]. Proper design of the front metallization (the size and shape), application of conductive pastes, determination of the emitter doping level, the morphology of the substrate, the adhesion of the metallization to the substrate are very important to minimize these losses [3]. The conditions for producing the material that is a solar cell or semiconductor structure depend on the source used [4]. Currently, numerous research institutions in the fields of electronics and photovoltaics are focused on the development and production of metal metallization using various methods (Figure 1) [5-12] with an emphasis on the applications of inkjet printing technology in the production of solar cells (Figure 2) [13]. In this method, metal inks are applied onto substrates in the form of droplets, which can be formed in two different ways. (mechanically by compressing the ink or by heating the ink) [14]. The study presented in [15] showcases the capability of producing highly efficient perovskite solar cells through digital inkjet printing. In study [16], the composition of ink was analyzed due to its impact on crystallization dynamics,

highlighting the importance of designing new types of ink systems for inkjet printing.

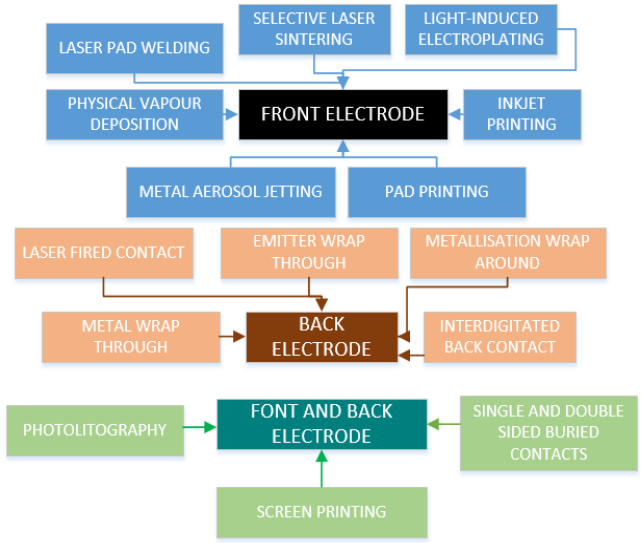

Fig. 1. Classification of manufacturing metal elements of solar cells [12]

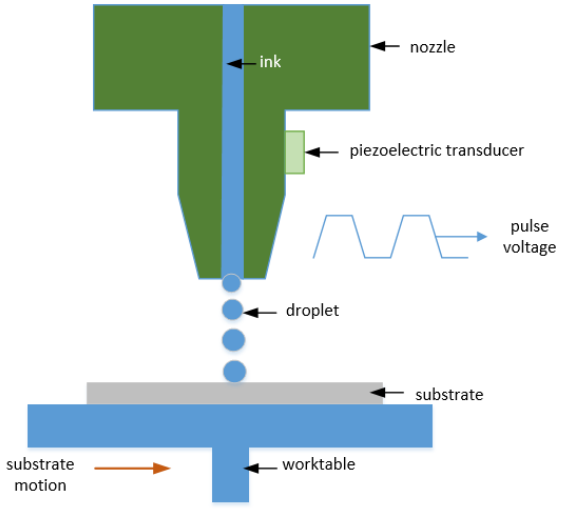

Fig. 2. Schematic of inkjet printer [13]

The significant technological advancements in solar cells require constant discoveries and research in their printing, power conversion efficiency, and stability. The papers [12, 17-23] describe other solar cell fabrication methods, including front and back metallization.

The analysis of the area of the photovoltaic market is used to verify and identify various factors that affect its development. One of these factors is the application of pastes in the production of solar cells. There are roughly 60 manufacturers of metallization pastes globally, playing a crucial role in the supply chain for solar cell producers, and a considerable portion of these manufacturers are based in China. Over 60% of companies engage in the production of silver pastes, while 25% focus on aluminum pastes and 5% on copper pastes. The remaining companies produce lead-free pastes and others (Fig. 3)[25].

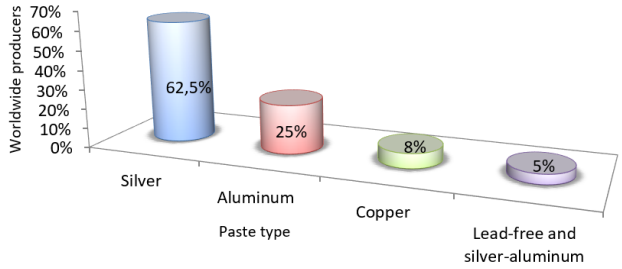

Fig. 3. Classification of metallization paste producers [24]

Materials science evolved, is inextricably linked with innovative measurement methods and the development of the latest technologies, including the technology of producing solar cells/semiconductor structures. These techniques are employed to specify pre-assembled devices such as photovoltaic cells/modules or cell components, which include front and rear contacts, for instance. These methods also characterise the materials used to manufacture semiconductor devices [4,26, 27].

The transmission line model (TLM) method (proposed by Shockley in 1964 [28], later modified by Berger [29, 30]) is a widely known and used method in the field of photovoltaics, as it is used to calculate and determine the electric parameter, i.e. the resistivity of the front contacts in silicon solar cells or conductive structures [31]. This method consists of forcing an electric current signal (I) between a selected pair of adjacent transmission lines of electrodes located on the surface of the investigated sample and measuring the voltage (U) on them [32]. The characteristics of the TLM method for measuring contact resistivity are thoroughly discussed in the work [33].

A central part of the work concerns the electrical properties of front metallization prepared in two series of classified samples. The criterion for selecting the conditions for producing the front metallization during deposition was based on the minimum resistivity ρ_c of the connection between the front electrode and the substrate. This work focuses on optimizing the experimental inks produced by an inkjet printer to manage this technological process. Additionally, major paste manufacturers are exploring a new market, including those already providing high-temperature silver pastes. Creating low-temperature pastes for solar cell construction necessitates a specific paste tailored for the front and rear contacts, considering its consumption and storage temperature. Paste manufacturers can meet such requirements thanks to cooperation with customers and research centres.

2. Research material

A total of fourteen samples were prepared for investigating. on a glass substrate deposited with indium tin oxide (ITO) at the Institute of Metallurgy and Materials Science of the Polish Academy of Sciences. The initial tests involved 12 samples in Series I and 16 samples in Series II. Table 1 presents example labels for the samples used in the preliminary experiments. Following these assessments, 6 samples were chosen for

additional testing from Series I, while 8 samples were selected from Series II. The sample designations in Series II were comparable to those in the Series I. The following series of samples with the front electrode was manufactured from the copper experimental paste marked X1 for the Series I and X2 for the Series II. The composition of the paste (functional phase, organic glaze, carrier and diluent). Selected components of the experimental paste are prepared under industrial conditions in the amount necessary to perform the printing process. Trade secrets cover other compositions of the paste. Both pastes were applied by inkjet printing and then dried in an oven at a low temperature.

The mentioned samples were prepared for the investigations: 25 cm^2 with a front electrode performed from two pastes, with three rows of front metallization elements on one test surface (Figure 4). Commercial base pastes from DuPont, marked as PV19B, were used to verify the operational parameters of the manufactured component K (Table 2). The prepared K component was dried and sieved, and then mixed with paste components to obtain a conductive paste. To create the barrier layer, electroless separation of nickel from a galvanic bath using a reducer was used. In order to obtain a suitable material for testing, copper powder available in industrial quantities, marked CNPC-FCU200, with an average copper grain diameter of 1 µm was selected as the base material. This material was covered with a barrier layer to obtain the K component, and the coating thickness was also optimized.

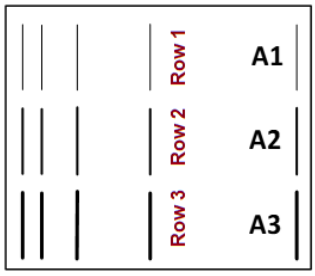

Fig. 4. Scheme of the path template for applying the front contacts of the investigated samples with an area of 25 cm^2 (where the size of the strips - front electrodes for the: A1 system: 0.1 x 8mm, A2 system: 0.2 x 8mm, A3 system: 0.3 x 8mm and the distance between them: 2.5; 5; 10; 20mm)

Table 1.

Samples labeled "Series I" that feature a front electrode composed of experimental paste X1 (where: electrode width - A1-3, I - current) chosen

No	Sample number	A1=0.01 cm, A2=0.02 cm, A3=0.03 cm	I, mA
1	1_1 1_2	0.01	10
			30
			50
		0.02	10
			30
			50
		0.03	10
			30
			50
2	2_1 2_2	0.01	10
			30
			50
		0.02	10
			30
			50
		0.03	10
			30
			50
3	3_1 3_2	0.01	10
			30
			50
		0.02	10
			30
			50
		0.03	10
			30
			50
4	4_1 4_2	0.01	10
			30
			50
		0.02	10
			30
			50
		0.03	10
			30
			50
5	5_1 5_2	0.01	10
			30
			50
		0.02	10
			30
			50
		0.03	10
			30
			50
6	6_1 6_2	0.01	10
			30
			50
		0.02	10
			30
			50
		0.03	10
			30
			50

Table 2.
Determination of the composition of experimental pastes and the weight and percentage of their individual ingredients

Number of sample series	Paste symbol	Paste ingredient	Ingredient share		Component symbol
			weight, g	percentage, %	
I	X1	component	20	50	K
		commercial paste	17	42	
		organic carrier	3	8	
II	X2	component	21	50	
		commercial paste	18	42	
		organic carrier	3	7	

3. Research Methodology

The electrical measurements of samples were performed using the test stand with patent number 219 794. Mainly, the contact resistance (R_c) and specific resistance (ρ_c) were determined by the "TLM" method. A detailed description of the method can be found in [26]. The publication [26] details the relationships based on which the resistivity and contact resistance are determined from the structure measurements shown in Figure 4. The investigations were performed for three settings of the current value: 10, 30, and 50 mA.

Examinations of the surface topography and cross-section of the produced front electrode, along with its junction with the substrate, were conducted using scanning electron microscopy.

4. Discussion of the research results

Figure 5 shows the results of resistance tests of 4 samples depending on the width of the applied electrode made of paste marked as X1. Based on the obtained electrical properties results, it can be concluded that for all 6 samples, the resistance results for the front electrodes are similar and repeatable (Figure 6).

Moreover, with this current value used, the measurement results obtained were the most repeatable. Correctly defining the layer resistance value complicates matters, because it is understood as a quantity characterizing the metal-semiconductor junction, considering the area above and below the junction. This resistance is determined between a selected pair of adjacent transmission lines of electrodes located on the surface of the tested sample. The characteristics of the phase boundary of the metal/semiconductor junction have played a key role since the beginning of semiconductor researches. A change occurs in the technological process of producing the connection between the substrate and the electrode. This change is related to the resistance value under the contact. The resistance of the metal on the contact line in this method is not considered. However, the key influence on the transmission of an electrical signal through a conductive line is the current flowing into the electrode line. The advantages of the TLM method include easy preparation of material for testing.

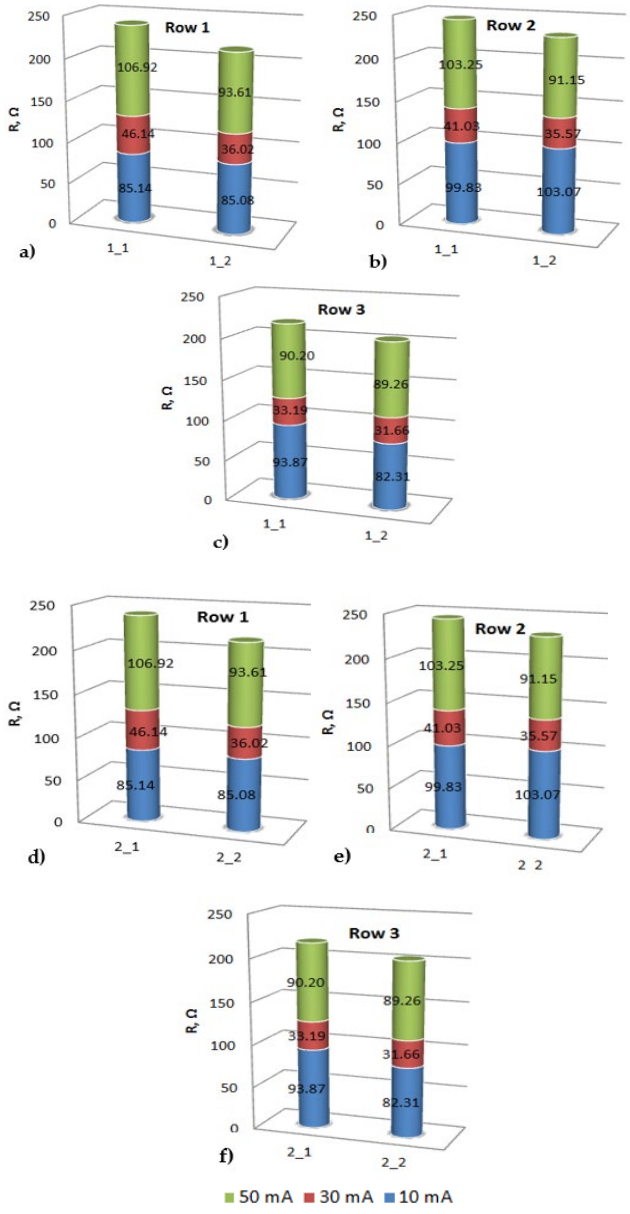

Fig. 5. Resistance of samples as a function of electrode width (where: row 1 = 0.01 cm, row 2 = 0.02 cm, row 3 = 0.03 cm) [24]

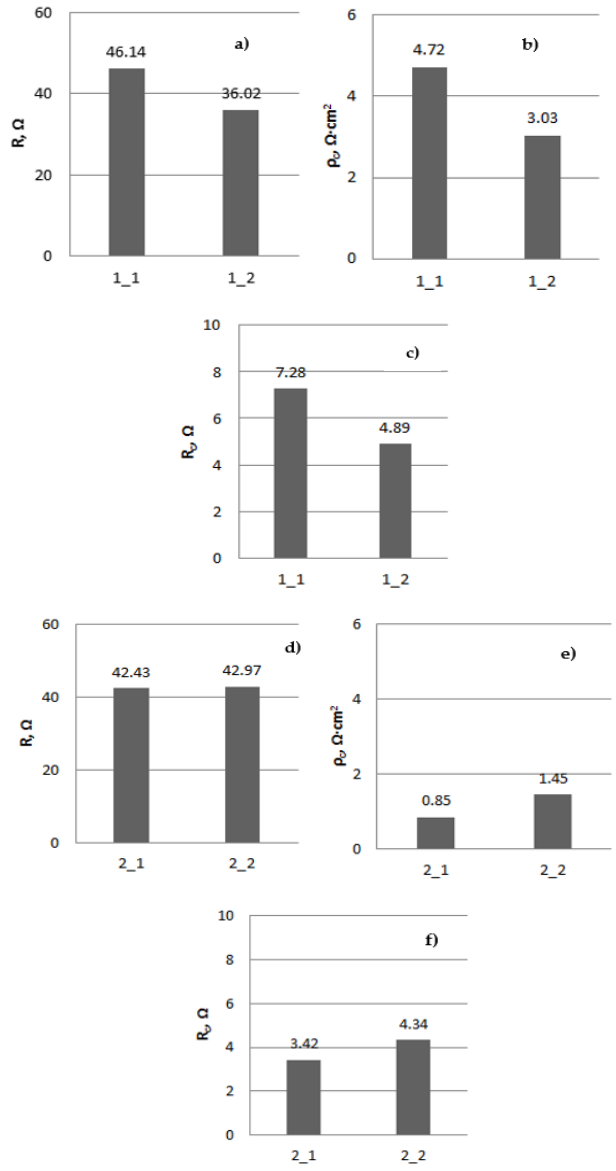

Fig. 6. The electrical parameters: resistance (R) (a, d), resistivity (ρ_c) (b, e), and contact resistance (R_c) (c, f) of the samples were measured at a current value of I=30 mA with an electrode width of 0.01 cm applied using a template and X1 paste

Figure 6 shows the results of testing the resistance of samples, resistivity and contact resistance at the metal-semiconductor interface depending on the width of the electrode made of paste marked as X1, obtained for a current value of 30 mA.

In the case of Figure 6 a, d, it can be concluded that the results of the resistance values for the tested row 1 of electrodes are comparable, and for four samples marked 1_1, 1_2, 2_1, 2_2 in the range of 36 ÷ 46 Ω. It should be noted that for two samples marked 1_1 and 1_2, there is a slight difference in the resistance value equal to 7 Ω, which may result from the front metallization process. In the case of Figure 6e, it can be stated that the lowest resistivity was obtained for the sample 2_1, 2_2 and the values, respectively, of 0.85 Ωcm^2 and 1.45 Ωcm^2. A slight difference in the obtained results of resistivity and contact resistance measurements may also result from the manual process of applying the front metallization. Based on the previously performed preliminary investigations, it was decided in the further part of the work to perform tests for the electrode width of 100 µm, and therefore, in the further research analysis, the results will be considered only for row 1 of electrodes, which is also with an electrode width of 100 µm. For samples 1_1 and 1_2, the resistivity values were 4.72 Ωcm^2 and 3.03 Ωcm^2 (Figure 6b), respectively, and the contact resistances for these samples were 7.28 and 4.89 Ω (Figure 6c). The sample 2_1 exhibited the lowest values of resistance and resistivity. The electrical values obtained by the TLM method for these samples are similar to those obtained for solar cells with front metallization made of commercial paste and co-fired in the high-temperature range, although made in the low-temperature range. A comparison of the results of electrical properties is presented in Table 3.

In addition, in the obtained results of electrical properties testing using the TLM method of all samples from the I series with front metallization on a glass substrate, the repeatability of the obtained results can be stated, as the linear nature of the regression relationship was found for all set current values in the range from 10 to 50 mA.

Figures 7 and 8 show surface observations in a scanning electron microscope of electrodes deposited from commercial and experimental paste on the investigated surfaces. Metallographic observations in a scanning electron microscope allow concluding the morphology of the electrode system deposited from a commercial paste and fired in a belt furnace at elevated temperature showing a porous structure containing a dense network of connections between grain agglomerates (Fig. 7b).

Table 3.
Comparison of chosen electrical parameters (R_c, ρ_c) of selected solar cells with front metallization applied from Du Pont PV19B commercial paste with paste from the X1 series, measured using the TLM method (for I=30 mA, R_p=50Ω/□, where T_M- co-firing temperature)

Sample symbol	Substrate type	R_c, Ω	ρ_c, Ωcm^2	T_M, °C
Z1	Silicon	6.24	3.95	900
Z2		5.63	3.33	915
Z3		4.97	3.28	930
1_1	Borosilicate glass	7.28	4.72	150
1_2		4.98	3.03	

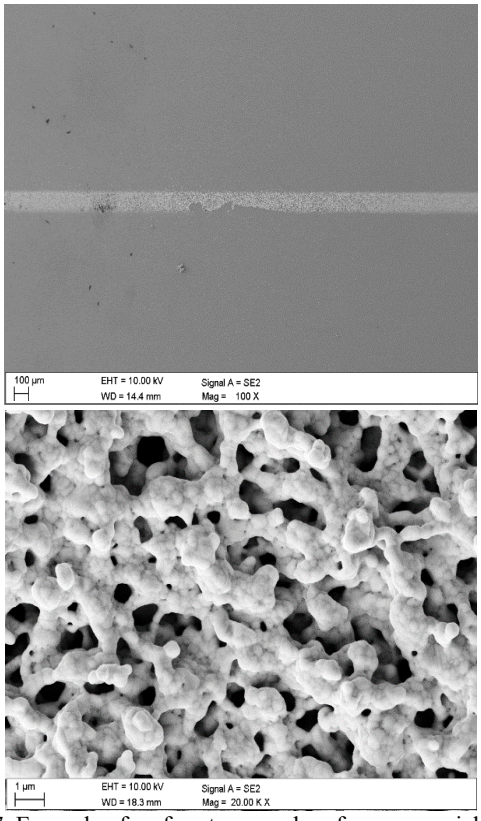

Fig. 7. Example of surface topography of a commercial paste layer on a glass substrate observed using SEM (sample Z3 from table 3)

In the case of the electrode system made of the experimental paste and co-fired in a belt furnace at a reduced temperature, it was found to have a similar porous structure containing a dense network of connections between grain agglomerates. Based on the experience gained and knowledge contained in the available literature, it is known that the obtained electrodes have a structure with a varying degree of density depending on the co-firing temperature.

Electrodes sintered in a high-temperature range usually have a more uniform structure obtained by melting n grains and their fusion. However, at low temperatures, they often show a non-uniform melted structure with irregular shapes. However, in the experiment, selected electrical parameters were measured for completely different structures - these were metal-semiconductor contacts for "classic" silicon solar cells using high-temperature conductive paste/silicon contacts and low-temperature conductive paste/ITO layer contacts, and similar resistivity and resistance values were obtained contact. The usefulness of the experimental pastes has been confirmed mainly by the quality of the layer topography (Figure 7 and 8) and the contact between the metal layer and the substrate.

Based on fractographic tests, it was found that electrodes made of commercial and experimental paste by firing in a belt furnace show homogeneous connections with the substrate, similar to a continuous connection (Fig. 9).

Figure 10 shows the results of the resistance investigations of 4 samples depending on the width of the applied electrode made of paste marked as X2. Based on the obtained electrical properties results, it can be concluded that for all 8 samples, the resistance results for the front electrodes are similar and repeatable. Slight differences in the values of the obtained test results may arise from the incorrect printing of the electrodes, which was associated with the smearing of the selective electrode or its lack.

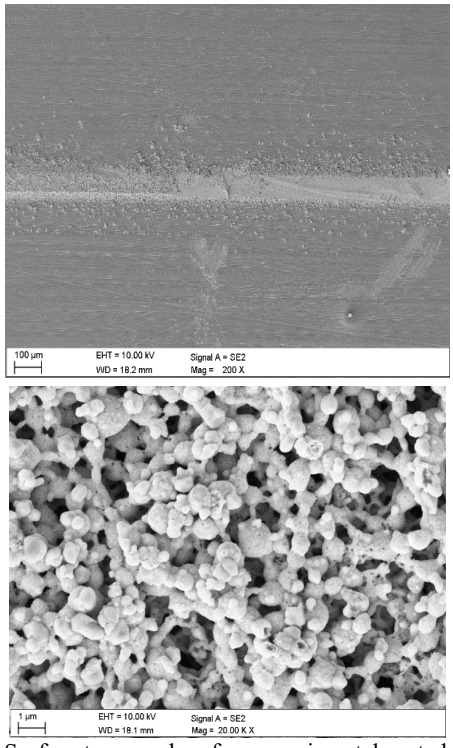

Fig. 8. Surface topography of an experimental paste layer on a glass surface (sample 1_2) observed using SEM

In addition, it can be stated that the resistance values measured for 10 and 50 mA are comparable and much higher than in the case of 30 mA; therefore, the results of tests for which the minimum value was obtained will be considered for further analysis, because this is the criterion for obtaining a good connection between the electrode and the tested substrate.

The electrical test results (for a current value of 30 mA) of the samples at the metal-semiconductor interface depending on the width of the applied electrode were made of X2 paste. It can be concluded that the resistance value result for row 1 of the electrodes for all samples is comparable (Figure 11). Slight differences in the result values from incorrect printing of the electrode lines. In the case of both resistivity and contact resistance results, it can be stated that the results are not repeatable because these values were negative in most of the analyzed results.

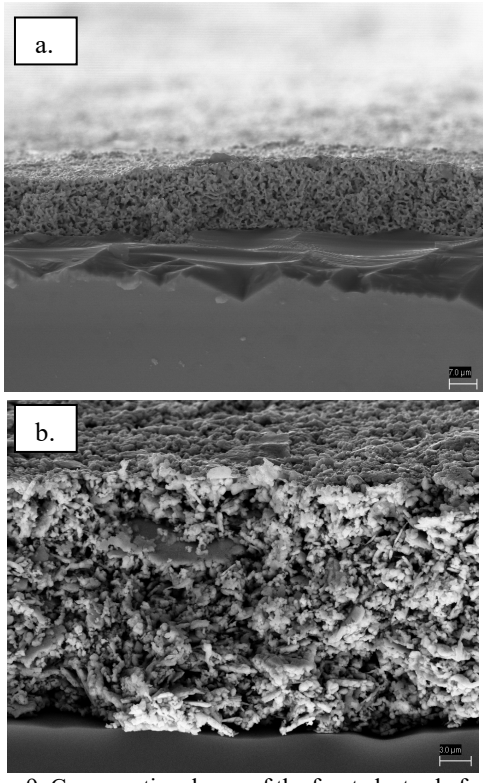

Fig. 9. Cross-sectional area of the front electrode from a) sample Z3 (Table 3) and b) sample 1_2 (Table 1)

In the obtained results of electrical properties testing using the TLM method of all samples from series I and II with front metallization on a glass substrate, the repeatability of the obtained results can be stated because the linear nature of the regression was found for all set current values in the range from 10 to 50 mA.

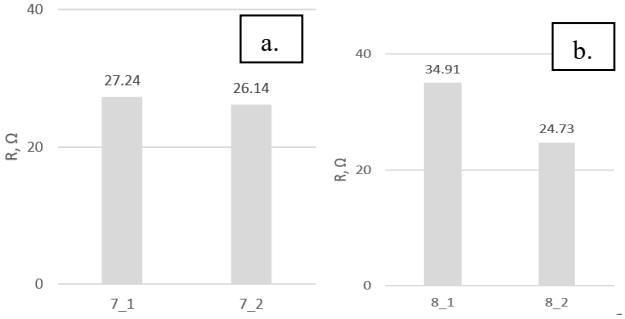

Fig. 10. Resistance (a, b) of the samples measured for the current value I=30 mA and the applied electrode width of 0.01 cm applied using a template and performed of X2 paste (an example)

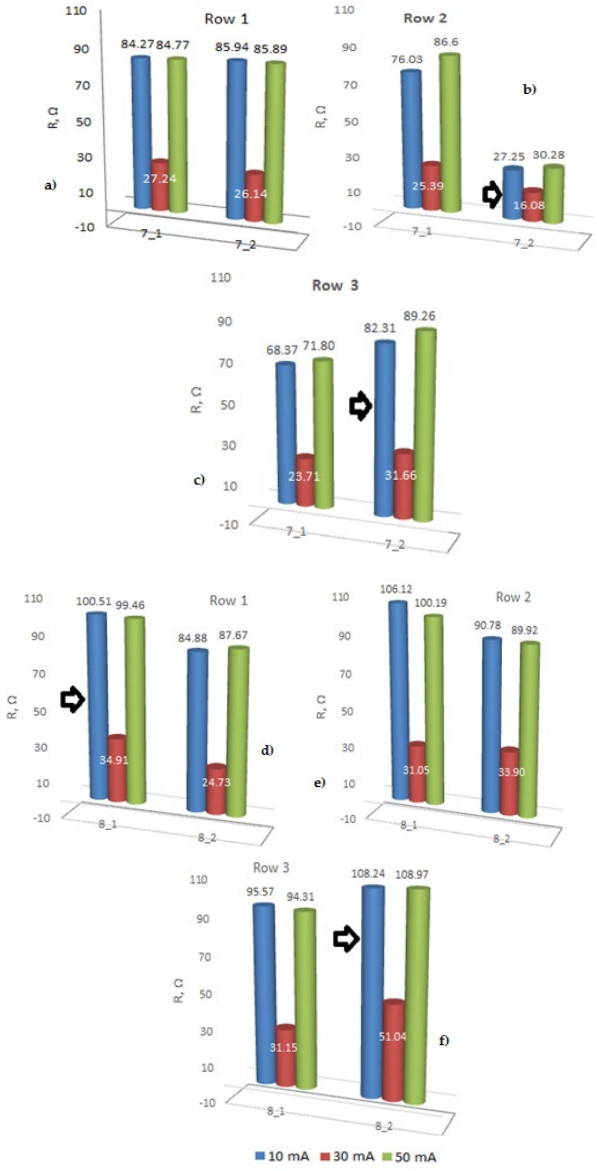

Fig. 11. Resistance of the samples (sample 7_1 and 7_2 (a-c), and samples 8_1 and 8_2 (d-f)) varies based on the electrode width (row 1, row 2, row 3) applied using a template and constructed with X2 paste (selected example).

5. Conclusions

Nowadays, scientific and research work in photovoltaics is focused on developing and producing electrical contacts using various techniques and determining the dependence of the resistivity of these contacts between multi-component metallic components and conductive layers [33]. The transmission line method determines the parameters characterising the solar cell contacts. It provides detailed information on the contact resistivity

value, i.e. the boundary layer between the metallic electrode and the solar cell emitter. A low resistance value means that the produced electrode has a uniformly molten structure and adheres well to the substrate, and a high resistance value means that the electrode has a non-uniform structure, e.g. containing numerous cracks and poorly adhering to the substrate. High resistivity may indicate that the contact could have been disturbed during the technological process, the space between the contact layer and the tested substrate was contaminated, or difficulties related to doping were encountered. The TLM method also has its advantages and disadvantages. The non-destructive method, the low cost of purchasing individual elements, the design of the stand itself, and its small dimensions are some of the advantages of the TLM method. The disadvantages include the adjustment of the line to the measurement points using linear regression, expressed by its slope value, which is subject to uncertainty and this is because, at the stage of making contact between the paste and the substrate, the contact layer resistance changes directly under the contact line [4].

Based on the analysis of the obtained investigations of electrical properties using the TLM, it can be concluded that in the case of the tested samples of the I series, repeatable results of the values of selected electrical parameters were obtained, including the resistance between the individual electrode distances, resistivity, and contact resistance. The smallest value of resistivity (3.03 Ωcm^2) and contact resistance (4.89 Ω) was obtained for sample 1_2. The electrical properties of the 1_1 and 1_2 front electrodes produced in the low-temperature range are similar to those of the PV19B front electrodes produced in the high-temperature processes. In addition, the repeatability of the test results was confirmed by the linear nature of the regression relationship for all set current values in the range of 10 to 50 mA. In the case of the II series, repeatable results of the values of selected electrical parameters were obtained, including the resistance between the individual distances of the electrodes. However, slight differences in the values result from incorrect printing of the electrode lines. Regarding the results of resistivity and contact resistance, it can be concluded that they are not repeatable, as the majority of the analyzed results were inconsistent. This inconsistency may be attributed to the non-uniformity of the pathways, particularly in areas where the pathways intersect the faults of the deposited layers, resulting in slightly reduced thickness over the faults. However, this aspect has not been examined further. However, the repeatability of the test results was confirmed by the linear nature of the regression dependence for all set current values in the range from 10 to 50 mA.

References

[1] Green, M.A. (1986). *Solar cells: operating principles, technology and system applications*. Englewood Cliffs, N.J.: Prentice-Hall Pub.

[2] Serreze, H.B. (1978). Optimizing solar cell performance by simultaneous consideration of grid pattern design and interconnect configurations. conference record. In Proceedings of 13th IEEE Photovoltaic Specialists Conference, Washington, D.C.

[3] Adamczewska, J. (1980). *Technological processes in semiconductor electronics*. WNT. (in Polish).

[4] Musztyfaga-Staszuk, M. (2022). *Application of the transmission line method (TLM) to measure the resistivity of contacts,* Gliwice: Silesian University of Technology Pub.

[5] Alemán, M., Streek. A., Regenfuβ, P., Mette, A., Ebert, R., Exner, H.; Glunz, S.W., Willeke G. (2006). Laser micro-sintering as a new metallization technique for silicon solar cells. In proceedings of the 21st European Photovoltaic Solar Energy Conference, 4 - 8 September 2006 (pp. 1-4). Dresden, Germany.

[6] Dross, F., Van, K.E.; Allebe, C., van der Heide, A., Szlufcik, J. Agostinelli G., Choulat P., Dekkers H.F.W., Beaucarne G. (2006). Impact of rear-surface passivation on MWT performances. Photovoltaic Energy Conversion. In proceedings of Conference Record of the IEEE 4th World Conference, 7 - 12 May 2006 (pp. 1291-1294). Waikoloa, Hawaii.

[7] Gautero, L., Hofmann, M., Rentsch, J., Lemke, A.; Mack, S., Seiffe, J., Nekarda, J., Biro, D., Wolf, A.; Bitnar, B., Sallese, J.M., Preu R. (2009). All-screen-printed 120-µm-thin large-area silicon solar cells applying dielectric rear passivation and laser-fired contacts reaching 18% efficiency. In proceedings of Photovoltaic Specialists Conference (PVSC), 34th IEEE, 7-12 June 2009 (pp. 001888-001893). Philadelphia, Pennsylvania.

[8] Ghozati, S.B., Ebong, A.U., Honsberg, C.B. & Wenham, S.R. (1998). Improved fill-factor for the double-sided buried-contact bifacial silicon solar cells. S*olar Energy Materials and Solar Cells*. 51(2), 121-128. https://doi.org/10.1016/S0927-0248(97)00210-9.

[9] Glunz, S.W. (2007). High-efficiency crystalline silicon solar cells. *Advances in Opto-Electrinics*. 1, 097370. https://doi.org/10.1155/2007/97370.

[10] Harder, N.P., Hermann, S., Merkle, A., Neubert, T., Brendemühl, T., Engelhart, P., Meyer, R. & Brendel, R. (2009). Laser-processed high-efficiency silicon RISE-EWT solar cells and characterization. *Physica Status, Solid*, *C*. 6(3), 736-743. https://doi.org/10.1002/pssc.200880720.

[11] Tepner, S. & Lorenz, A. (2023). Printing technologies for silicon solar cell metallization: Acomprehensive review. *Progress in Photovoltaics: Research and Applications*. 31(6), 557-590. https://doi.org/10.1002/pip.3674.

[12] Musztyfaga, M. (2011). *Laser micromachining of silicon elements photovoltaic cells 2011.* Silesian University of Technology, Gliwice.

[13] Hunde, B.R. & Woldeyohannes A.D. (2023). 3D printing and solar cell fabrication methods: A review of challenges, opportunities, and future prospects. *Results in Optics*. 11, 100385, 1-11. https://doi.org/10.1016/j.rio.2023.100385.

[14] Lin, X., Kavalakkatt, J., Lux-Steiner, M.C. Ennaoui, A. (2015). Inkjet-printed Cu2ZnSn (S, Se) 4 solar cells. *Advanced Science.* 2(6), 1500028.

[15] Mathies, F., Eggers, H., Richards, B.S., Hernandez-Sosa, G., Lemmer, U. & Paetzold, U.W. (2018). Inkjet-printed triple cation perovskite solar cells. *ACS Applied Energy Materials*. 1(5), 1834-1839. https://doi.org/10.1021/acsaem.8b00222.

[16] Li, Z., Li, P., Chen, G., Cheng, Y., Pi, X., Yu, X. & Song, Y. (2020). Ink engineering of inkjet printing perovskite. *ACS*

Appl. Mater. Interfaces. 12(35), 39082-39091. https://doi.org/10.1021/acsami.0c09485.
[17] Nagarajan, B., Raval M., C. & Saravanan, S. (2019). Review on Metallization in Crystalline Silicon Solar Cells. *In Solar Cells*. (1st ed.). London: The Intech Open Ltd Pub.
[18] Wenham, S.R., Green, MA. (1986). Patent no 4,626,613. US.
[19] Romain, C., Mohamed, A. & Mustapha, L. (2013). Improvement of back surface metallization in a silicon interdigitated back contacts solar cell. *Energy Procedia.* 38, 684-690. https://doi.org/10.1016/j.egypro.2013.07.333.
[20] Ehling, C., Schubert, M.B., Merz, R., Müller, J., Hlusiak, M., Rostan, P. J. & Werner, J. H. (2009). 0.4% absolute efficiency gain by novel back contact. *Solar Energy Materials & Solar Cells.* 93(6-7), 707-709. https://doi.org/10.1016/j.solmat.2008.09.036.
[21] Erath, D., Filipović, A., Retzlaff, M., Goetz, A.K., Clement, F., Biro, D. & Preu, R. (2010). Advanced screen printing technique for high definition front side metallization of crystalline silicon solar cells. *Solar Energy Materials & Solar Cells.* 94(1), 57-61. https://doi.org/10.1016/j.solmat.2009.05.018.
[22] Kopecek, R., Buchholz, F., Mihailetchi, V.D., Libal, J., Lossen, J., Chen, N., Chu, H., Peter, C., Timofte, T., Halm, A. et al. (2023). Interdigitated back contact technology as final evolution for industrial crystalline single-junction silicon solar cell. *Solar.* 3(1), 1-14. https://doi.org/10.3390/solar3010001.
[23] Glunz, S. W., Preu, R., Schaefer, S., Schneiderlochner, E., Pfleging, W., Ludemann, R. & Willeke, G. (2000). New simplified methods for patterning the rear contact of RP-PERC high-efficiency solar cells. In proceedings of 28th IEEE PVSC, Anchorage, Alaska; 15-22 September 2000 (pp. 168-171).
[24] ENF Solar. (2024). Retrieved December, 2022, from https://www.enfsolar.com/directory/material/metallization_paste?tech=408
[25] Retrieved November, 2022, from http://taiyangnews.info/TaiyangNews_Market_Survey_Metallization_Pastes_2019_20_download_v1.pdf.
[26] Musztyfaga-Staszuk, M. (2019). *New copper-based composites for silicon photovoltaic cells*. Gliwice: Silesian University of Technology Pub.
[27] Goetzberger, A., Scarlett, R. M. & Shockley, W. (1964). *Research and investigation of inverse epitaxial UHF power transistors*. Air Force Avionics Lab., Wright-Patterson Air Force Base, OH, USA, Rep. AD0605376.
[28] Defense Technical Information Center. (2025). Retrieved November 2022, from https://apps.dtic.mil/sti/citations/AD0605376
[29] Berger, H.H. (1969). Contact resistance on diffused resistors. In IEEE Solid-State Circuits Conference. Digest of Technical Papers (pp.160–161).
[30] Berger H.H. (1972). Models for contacts to planar devices. *Solid State Electron.* 15(2), 145-158. https://doi.org/10.1016/0038-1101(72)90048-2.
[31] Denhoff, M.W., Droleta, N. (2009). The effect of the front contact sheet resistance on solar cell performance. *Solar Energy Materials and Solar Cells.* 93(9), 1499-1506. https://doi.org/10.1016/j.solmat.2009.03.028.
[32] Schroder D.K. (2006). *Semiconductor material and device characterization (3rd ed.).* Arizona State University Tempe, AZ. In IEEE Press and John Wiley & Sons Inc.
[33] Pysch, D., Mette, A., Filipovic, A., Glunz, S.W.A. (2009). Comprehensive analysis of advanced solar cell contacts consisting of printed fine-line seed layers thickened by silver plating. *Progress in photovoltaics: Research and Applications*. 17, 101-114. https://doi.org/10.1002/pip.855.